LATE TIME OPTICAL SPECTRA FROM THE Ni^{56} MODEL FOR TYPE I SUPERNOVAE

Tim S. Axelrod

THIS PAPER WAS PREPARED FOR SUBMITTAL TO
THE PROCEEDINGS OF
THE SUPERNOVA TYPE I WORKSHOP
UNIVERSITY OF TEXAS, AUSTIN, TX
17-19 March 1980

April 1980

Lawrence Livermore Laboratory

LATE TIME OPTICAL SPECTRA FROM THE
Ni^{56} MODEL FOR TYPE I SUPERNOVAE

Tim S. Axelrod

Lawrence Livermore Laboratory, University of California
Livermore, California   94550

The hypothesis that the exponential tail of the SNI lightcurve is powered by the beta decay chain $Ni^{56} \to Co^{56} \to Fe^{56}$ was apparently first proposed by Truran in 1967. Recently, Arnett (1979), and Colgate, Petshek, and Kriese (1979), have investigated the energy deposition from the gamma rays and positrons emitted by this decay chain in a homologously expanding uniform sphere, and shown that with the additional assumption that the deposited energy is radiated as optical light with unit efficiency, the SNI light curve can be accurately reproduced if $M/V_9^2 \approx 0.2$, where M is the mass of the sphere in $M_\odot$, and $V_9 \times 10^9$ cm/sec its expansion velocity. Meyerott (1978, 1979) has considered the problem of generating the optical spectrum in such a model, and shown both that high conversion efficiency from deposited gamma rays into optical light is possible, and that, with a particular choice for the

temperature and ionization state, the most prominent features
observed in the late-time spectra of SN1972e can be reproduced. It
is not clear, however, that the selected temperature and ionization
state are consistent with one another, and still less clear that
they are consistent with the parameters chosen by Colgate et al to
fit the light curve. Furthermore, an important prediction of the
Ni^{56} model remains untested: that the late time spectra should
show evidence for the abundance of Co decaying with the proper 118
day mean life of Co^{56}.

In an attempt to answer these questions, a numerical model has
been created that produces self-consistent optical spectra, tempera-
tures, and ionization states for a homologously expanding spherical
shell which at t = 0 is assumed to consist of pure Ni^{56}, and is
further assumed to have density independent of radius within the
shell. In this case, the output of the numerical model is deter-
mined by only three variable parameters: M, the mass of the shell
in units of $M_{\odot}$; V_9, the velocity of the outer edge of the shell
in units of 10^9 cm/sec; and h, the ratio of the shell thickness to
the outer radius. The physics and numerical methods used in this
model are described in detail elsewhere (Axelrod 1980). A brief
summary is given here, followed by some results from the calcula-
tions.

The first step of the calculation consists of determining the
fraction of the decay energy deposited in the shell. For the gamma
rays, which account for 96% of the Co^{56} decay energy, the problem

is straightforward, and the method used is equivalent to that of Colgate et al. The fate of the remaining 4% of the energy which is emitted as positrons is considerably less certain, due to the strong effect of very weak magnetic fields on positron transport. As first pointed out by Arnett (1979), the luminosity at late times (t ≳ 200 days) is dominated by the positrons, due to their much shorter deposition range, and therefore the nature of their transport has an important effect on the late time light curve. In contrast to Arnett and Colgate, both of whom assume that the positrons are free to escape, I have made the opposite assumption, namely that the positrons are trapped by magnetic fields and deposit all their energy in the nebula. While the reasons for this choice are not compelling, it may be noted that the gyroradius of a 1 MeV positron in a typical interstellar field of 1×10^{-6} gauss is 5×10^{9} cm, while the characteristic size of the nebula is about 10^{16} cm. Additionally the presence of turbulent motions in the nebula is likely to be reflected in a turbulent magnetic field so that escape along field lines seems improbable.

A wide variety of processes is involved in absorption of the energy possessed by the energetic (E ≈ 1 MeV) electrons which result from the Compton scattering of decay gamma rays, and by the decay positrons, which have comparable energies. The most important of these processes and their interrelationship are shown in Figure 1. The excitation branch is particularly complex, due to the very large number of excitations possible in the lower ionization stages of Fe,

and it is not treated in detail. Instead, it is recognized that the states which are most likely to be excited are those which decay by Auger processes or by emission of ultraviolet photons. In the case of Auger decay, the resulting electrons are of low enough energy that they transfer their energy predominantly to the thermal electron gas, as is also the case for the secondary electrons resulting from collisional ionizations. In the case of radiative decay, the bound-free optical depth for the resulting ultraviolet photons is typcially large, so that the energy is transferred into ionization, and heating of the electron gas by the resulting secondary. To first order, then, one may ignore the excitation branch and force all the primary energy to flow down the collisional ionization and thermal heating branches with a somewhat changed branching ratio. It would be worthwhile to investigate this approximation more fully, but it is difficult due to the absence of most of the required excitation crossections.

The ionization state is determined by requiring that the rate of collisional ionization by primaries be balanced by radiative recombination as modified by reabsorption of the recombination radiation. This may be written as:

$$\gamma_i f_i = n_e \alpha_{i+1}(T_e) \, f_{i+1}$$

where γ_i is the ionization rate of the ith ion (i = 0, ..., Z), f_i is the fractional abundance of the ith ion, and α_i is the

recombination coefficient, which depends not only on the electron temperature, T_e, but also implicitly on the set of f_i's due to reabsorption effects. n_e is the electron density and is given by

$$n_e = n_0 \sum_i i f_i$$

where n_0 is the ion density.

The electron temperature, which must be solved for simultaneously with the ionization state, is set by requiring the energy deposition rate into the thermal electrons be balanced by radiative losses from states excited by collisions with the thermals, so that

$$\dot{\varepsilon}_{th} = n_e \sum_i f_i L_i(T_e, n_e)$$

Here L_i is the cooling function for the ith ion, and its determination requires calculation of level populations, which are in general far from LTE. A typcial cooling curve is shown in Figure 2. It is important to notice that a small drop in the value of L_i required for thermal balance, whether due to a drop in $\dot{\varepsilon}_{th}$, or to an increase in n_e, may result in an almost discontinuous drop in T_e by a large factor. In the subsequent discussion this will be referred to as the "infrared catastrophe" (IRC), since it results in the entire luminosity being radiated by infrared transitions with $\lambda > 20 \ \mu$.

The existence of the IRC has important implications for calculations of both light curves and spectra. Consider, in particular, the effect of a non-constant density profile on the optical light curve. At late times, the densities are low enough that the cooling curves are nearly independent of n_e. This is also the case for $\dot{\epsilon}_{th}$, which is simply the deposition rate from decays (which is independent of density at late times when positrons, which are locally deposited, dominate) times an efficiency factor which has been found to have the nearly constant value 0.95. In this case the spatial dependence of T_e is determined by

$$L(T_e(r)) \approx \frac{\dot{\epsilon}_{th}(t)}{n_e(r)}$$

If $n_e(r)$ decreases monotonically with radius, there is a critical radius inside of which IRC has occurred, so that that portion of the nebula is invisible in the optical. The density profile is then reflected directly in the optical light curve as the critical radius sweeps outward through the nebula. Detailed calculations have verified this simple picture, and indicate that realistic density profiles may reproduce the observed SNI optical light curve during the exponential tail phase without having recourse to positron escape.

Having completed the determination of the electron temperature and ionization state, the final step of the calculation is the computation of the emergent spectrum. This is complicated by the fact that significant line opacity remains in some spectral regions, predominently originating from low levels of FeI. At the times of interest, the fractional abundance of FeI is typcially less than 10^{-3}, so that collisional excitation of these lines is negligible in comparison with forbidden lines originating from the much more abundant FeII and III. Their importance arises from the fact that the allowed lines may absorb photons emitted at a higher frequency and redshifted into resonance as they travel through the $\vec{V} = K\vec{R}$ velocity field. Following such an absorption, reemission may occur at any of several frequencies equal to or less than the absorption frequency, since most of the states excited have several possible radiative decays. In this manner, the allowed lines significantly redistribute the forbidden line emission spectrum. With this exception, the spectrum calculation is straightforward, consisting of a sum over the lines of each level, with line profiles appropriate for the assumed spherical shell.

An extensive series of these calculations have been performed with the goal of finding the region of parameter space which gives both spectra and light curves in agreement with observations, the well observed SN1972e being used as reference. An example of the agreement obtainable is shown in Figure 3, where the synthetic spectrum from a shell with $M = 0.8$, $V_9 = 0.7$, and $h = .17$ is shown

superimposed on the SN1972e spectrum at a time 255 days after explosion. A Co abundance of 0.1 has been assumed, as expected from the Ni^{56} model for this time. It is important to note that the IRC is not a factor at this time for reasonable density profiles, so that the errors made by the constant density shell approximation are not yet severe. The evidence for the presence of Co at this time is quite strong, as shown in Figure 4, and later spectra are consistent with the Co abundance decreasing at the expected rate. Unfortunately, the radiative rates for Co are quite poorly known, and definitive results on the Co abundance must wait for better atomic data.

The results of these calculations have made it clear that models with proper light curves may have optical spectra which are in gross disagreement with the observations, and that in general the light curve shape imposes very weak constraints on the shell parameters. The optical spectrum is found to depend on two principal parameters: the ion density, which determines the temperature and ionization state; and the shell velocity, which determines the shape of spectral features through the lineshapes. If one chooses a family of models with the same density profiles (the same value of h in the case of shell models), one can then define a class of models, labelled by the Ni^{56} mass and expansion velocity at the edge of the Ni^{56} core, which give approximately correct optical spectra. Such a class is shown in Figure 5. It is apparently that many proposed SNI models fall well outside the acceptable area of

parameter space, for example the Colgate model, which was chosen to fit the light curve. Chevalier (1980) and Weaver (1980), however, have both proposed models which do fall in the acceptable area, and therefore may be expected to generate optical spectra similar to those observed. Although the limits that have been defined depend on the density profile assumed, the dependence is fairly weak, so that the results have general applicability.

Future work will incorporate the effects of the density profile on the optical spectra and will therefore be applicable at later times when the IRC becomes effective and the current shell model fails. Particularly if the necessary atomic data becomes available (especially Fe collision strengths and Co radiative rates), a fairly complete reconstruction of the density profile and mass of SN1972e should be possible.

References

1. Arnett, W. D., 1979, Ap. J. (Letters), 230, L37.

2. Axelrod, T. S., 1980, in preparation.

3. Branch, D., 1980, preprint.

4. Chevalier, R. A., 1980, Texas Workshop on Type I Supernovae, Austin, TX.

5. Colgate, S. A., Petschek, A. G., and Kriese, J. T., 1979, preprint.

6. Kirshner, R. P. and Oke, J. B. 1975, Ap. J., 200, 574.

7. Meyerott, R. E., 1978, Ap. J. 221, 975

   _____ 1979, preprint.

8. Weaver, T. A. 1980, Texas Workshop on Type I Supernovae, Austin TX.

Figure Captions

Fig. 1   Major pathways for deposition of the primary electron energy.

Fig. 2   Cooling curve for FeII at $n_e = 10^5$

Fig. 3   The observed spectrum of SN1972e 255 days after explosion is shown by a solid line (Kirshner and Oke 1975). The synthetic spectrum is shown by the dashed line. The shell parameters are M = 0.8, V_9 = 0.7, and h = .17, with M_{co}/M = 0.1. The resulting temperature and ionization state is T_e = 6100 K, f_0 = 1.2 x 10^{-4}, f_1 = 1.3 x 10^{-1}, f_2 = 5.3 x 10^{-1}, f_3 = 3.0 x 10^{-1}, f_4 = 3.7 x 10^{-2}, f_5 = 1.8 x 10^{-3}.

Fig. 4   Same as for Fig. 3 but the contribution of CoIII to the synthetic spectrum is shown by the dashed line. The most prominent lines arise from the a^2G multiplet of Co III.

Fig. 5   Models which produce late time optical spectra similar to SN1972e fall within the hatched area. Branch (1980) has set an upper limit on V_9 of 0.8, shown by the vertical dashed line and this further restricts models to the doubly hatched area. Uniform spheres with E = 10^{51} ergs fall on the dashed curve.
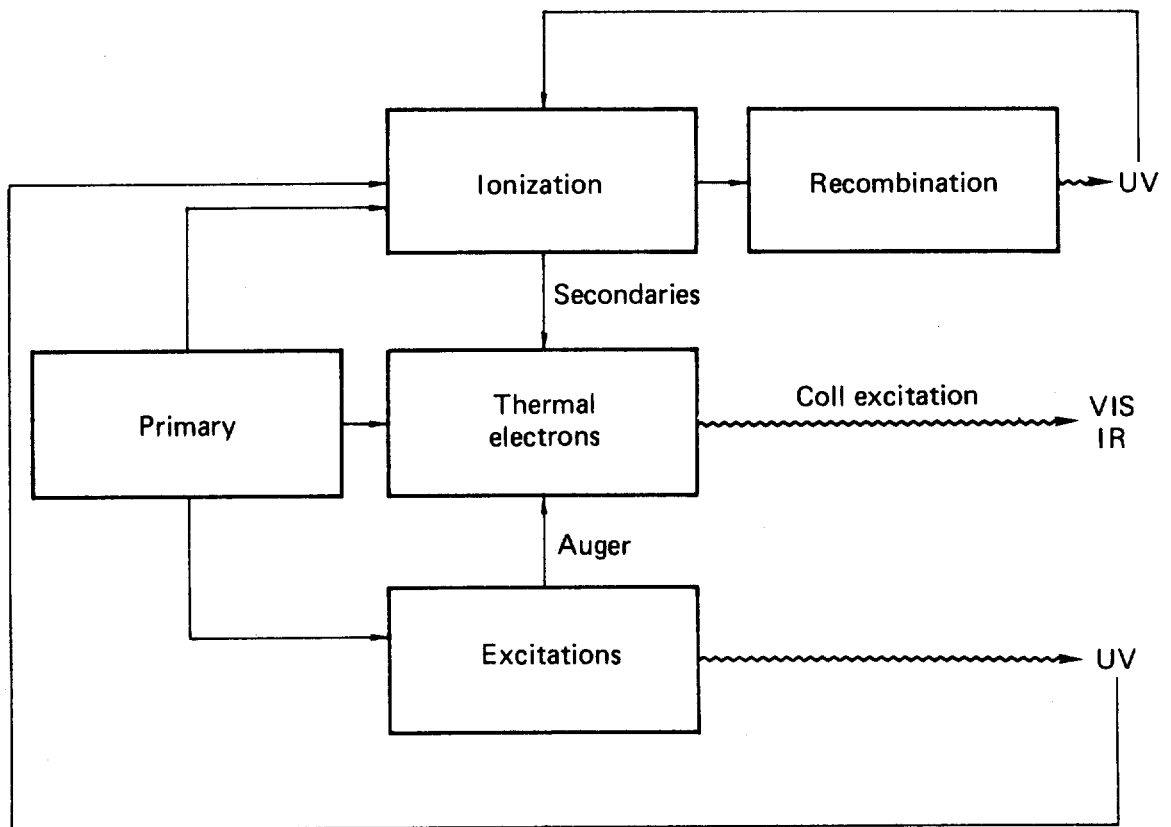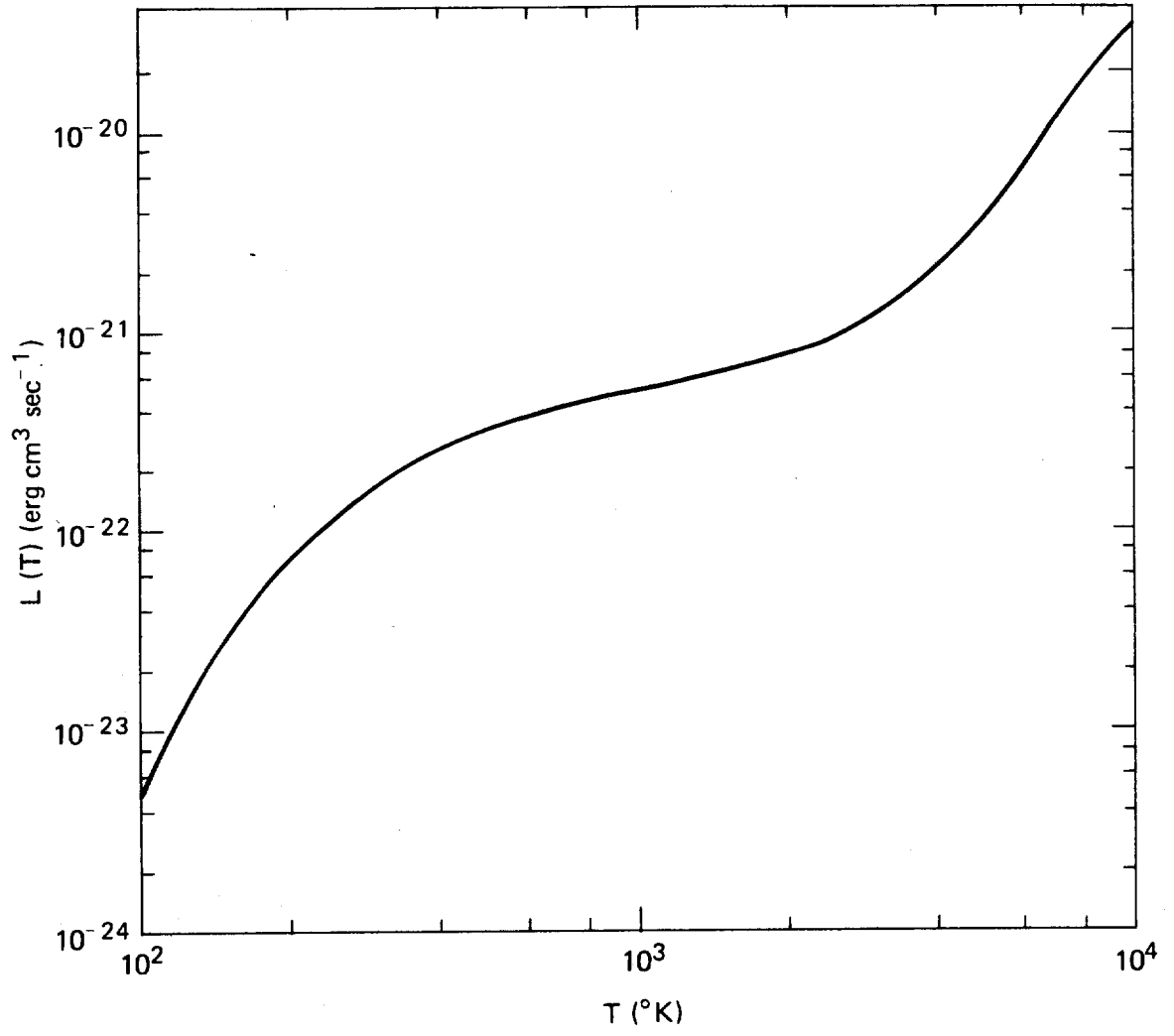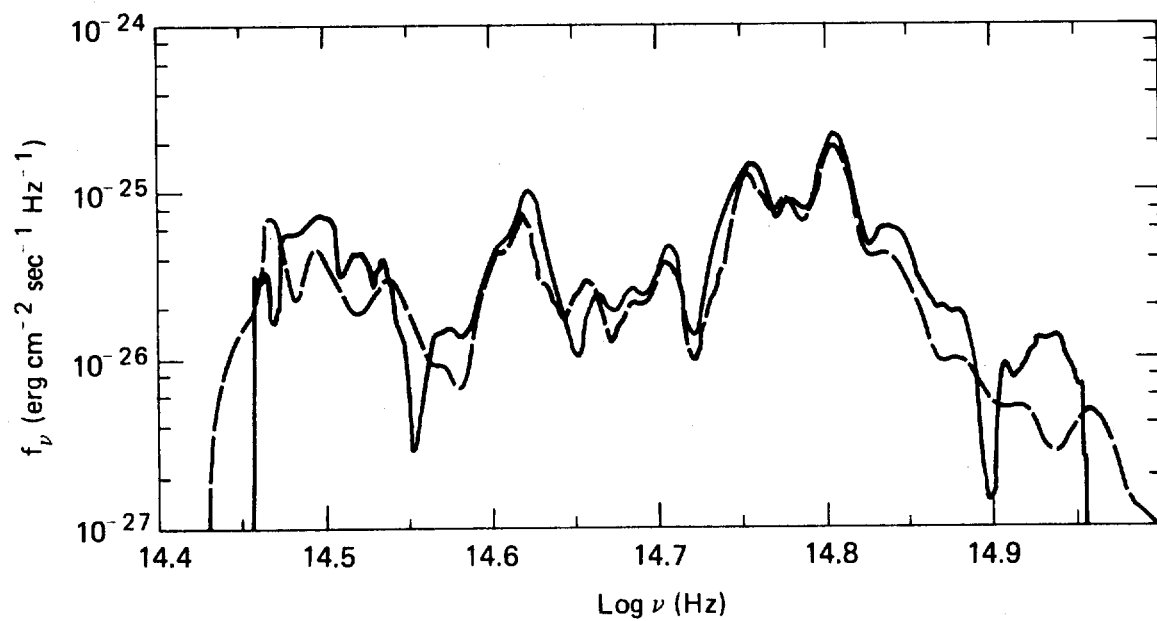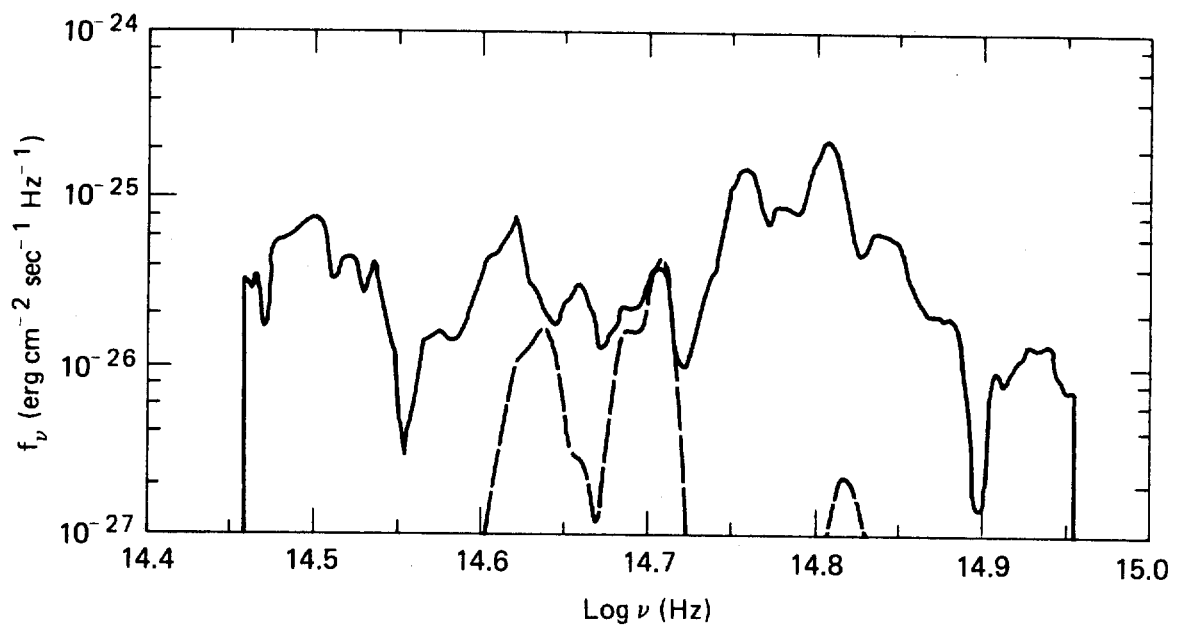
Figure 1

Figure 2

Figure 3

Figure 4

Figure 5